Orthodontics & Craniofacial Research

SPECIAL ISSUE Facial Orthopedics With Skeletal Anchorage

WILEY

RESEARCH ARTICLE OPEN ACCESS

Investigation of Effects of Hybrid Hyrax-Mentoplate Treatment in High-Angle Class III Patients: A Three-Dimensional, Retrospective Study

Gamze Yıldırım[1] | Elvan Önem Özbilen[1] | Fulya Özdemir[2]

[1]Department of Orthodontics, Faculty of Dentistry, Marmara University, Istanbul, Turkey | [2]Department of Orthodontics, Faculty of Dentistry, Istanbul Health and Technology University, Istanbul, Turkey

Correspondence: Gamze Yıldırım (gamze.yildirim@marmara.edu.tr)

Received: 27 June 2025 | **Revised:** 2 April 2026 | **Accepted:** 3 August 2026

Keywords: Class III orthopaedic treatment | high-angle vertical pattern | hybrid-hyrax

ABSTRACT

Objective: This retrospective study evaluated three-dimensional effects of hybrid hyrax-mentoplate (HH-M) orthopaedic treatment in high-angle Class III individuals using Cone Beam Computed Tomography (CBCT) images.

Materials and Methods: Pre-treatment (T0) and post-treatment (T1) CBCTs of 17 fully compliant high-angle Class III patients (7 males, 10 females, age: 11.7 ± 1.32 years, treatment duration: 12.62 ± 1.7 months) treated with HH-M were analysed. T0 and T1 CBCTs were superimposed from the cranial base using artificial intelligence-based AMASSS module of the 3D Slicer version 5.8.1 software (www.slicer.org). Linear and angular changes were analysed in the sagittal, vertical and transverse planes, alongside three-dimensional landmark displacements and volumetric airway measurements. Significance level was set at $p < 0.05$.

Results: Significant increases occurred in SNA, ANB and Occlusal Plane (OP) to Mandibular Plane (MP) angle ($p < 0.001$, $p < 0.001$, $p = 0.001$, respectively), while Sella-Nasion to OP and Palatal Plane (PP) to OP decreased ($p = 0.008$, $p = 0.008$, respectively). Vertical linear measurements remained stable ($p > 0.05$). All transverse linear measurements increased ($p < 0.05$). Upper Molar (UM) to PP, Upper Incisor to PP, Lower Incisor to MP and overjet have significantly increased ($p < 0.001$, $p = 0.018$, $p = 0.048$, $p < 0.001$, respectively). Overbite remained unchanged ($p > 0.05$). Nasopharynx ($p = 0.008$) and Middle Pharynx ($p = 0.003$) volumes significantly increased.

Conclusion: Despite the significant alterations observed in OP and UM-PP, this technique effectively managed to maintain overall vertical skeletal dimensions without inducing a significant change in other facial height parameters and enhanced the airway volume. Significant expansion occurred across maxillary, nasal and zygomatic levels. HH-M represents an effective orthopaedic treatment approach for high-angle Class III patients.

1 | Introduction

Skeletal Class III treatment in growing subjects is challenging due to unpredictable growth patterns, remaining growth potential and varying eligibility for different treatment protocols [1, 2].

Those patients frequently present with sagittal maxillary retrusion and transverse deficiency [3]. To address this and mobilize circummaxillary sutures for greater orthopaedic advancement, Rapid Palatal Expansion (RPE) is performed prior to or concurrent with Facemask (FM) protraction in traditional protocol [2, 4]. However, the abovementioned appliances are tooth-borne in nature and cause undesirable dentoalveolar side effects alongside skeletal changes [5, 6]. To overcome this limitation clinicians increasingly rely on skeletal anchorage and current protocols include applying forces between FM and miniplates or hybrid hyrax (HH), or between mentoplate (M) and HH or zygomatic miniplates [3, 7–9].

Although the early mixed dentition phase is considered the optimal period for maxillary protraction, skeletal anchorage-supported hybrid methods have been reported as a feasible alternative capable of producing significant skeletal changes in patients treated beyond early stage [10, 11].

Patients with a high-angle growth pattern represent a more challenging subgroup, as they are inherently more susceptible to undesirable vertical increases often associated with conventional techniques. A key advantage of skeletal anchorage in Class III treatment is the maintenance of vertical facial height, thereby expanding the pool of patients eligible for orthopaedic intervention [1, 3, 9–11]. Given that vertical facial height remains almost unchanged following HH-M, this approach offers a viable option for high-angle patients [1, 3, 9]. The favourable vertical control observed with the HH-M technique arises primarily from the combined biomechanical effect of its skeletal anchorage components.

Studies examining the impact of Class III orthopaedic treatments on airway report controversial outcomes [12–15]. While a study performing linear two-dimensional (2D) measurements with HH-M technique found non-significant alterations in nasopharyngeal airway at the adenoidal level [16], another study using Miniscrew-Anchored Maxillary Protraction (MAMP) reported significant increase in oropharyngeal airway volume three-dimensionally (3D) [12].

This study aimed to evaluate the skeletal, dental, soft tissue and airway effects of HH-M appliance in high-angle Class III patients using Cone Beam Computed Tomography (CBCT) images. Although the primary investigation centres on vertical facial height and airway dimensions, additional parameters were analysed for a comprehensive evaluation of treatment effects. The first hypothesis was that HH-M appliance would not affect facial height in high-angle Class III patients, while the second hypothesis was that it would increase airway volume.

2 | Materials and Methods

2.1 | Study Design and Setting

This retrospective study was approved by the Ethical Committee of Marmara University, Faculty of Medicine (Protocol no: 09.2023.1237, 06.10.2023). Records of patients treated between 2018 and 2023, including initial intraoral-extraoral photographs and lateral cephalometric radiographs, were retrieved from the archive of Marmara University, Department of Orthodontics.

2.2 | Sample Size Calculation

Sample size calculation was performed using G*Power software (version 3.1.9.7; Heinrich-Heine-Universität Düsseldorf, Germany). Based on SNA angle alterations reported in a previous study (T0: 79.23° ± 3.08°, T1: 81.47° ± 3.15°), power analysis was conducted using a paired-sample *t*-test. To achieve a statistical power of 80% with an α of 0.05 and an effect size of 0.71, it was determined that a minimum of 14 patients was required. To further enhance the reliability and accommodate potential data loss, 17 patients were included [9].

2.3 | Participants

Inclusion criteria were: skeletal Class III malocclusion (SNA < 80°, ANB ≤ 0) and high-angle vertical growth pattern (Sella-Nasion (SN) to Mandibular Plane (MP) angle > 39°) according to T0 CBCT measurement, concave profile, treated with HH-M, individuals who underwent 1-week expansion, complete patient files, photographs, and CBCT records. Exclusion criteria were: missing patient files, photographs and CBCT records, non-cooperative patients, craniofacial deformity, growth or hormonal disorder, history of previous orthodontic treatment. From 32 individuals, 15 patients were excluded from study group due to non-compliance with treatment (4), incomplete archive records (2), and not meeting inclusion criteria (9). Records of 17 patients (7 males, 10 females, age: 11.7 ± 1.32 years, Table 1) who met the inclusion criteria were retrieved from the archive. Parents or legal guardians of all patients signed a written informed consent before treatment.

While a subset of this cohort appeared in preliminary studies evaluating basic dentoskeletal measurements ($n = 6$) [17], and maxillary molar changes ($n = 10$) [18], the current investigation is entirely distinct. It expands the sample to 17 patients and utilizes artificial intelligence (AI)–based, voxel-based superimposition to evaluate total 3D displacements, transverse expansion, soft tissue and airway alterations—none of which were previously addressed.

2.4 | Treatment Protocol

In all patients, two 1.7 × 8 mm (OrthoEasy Pal Forestadent, Bernhard Foerster GmbH, Pforzheim, Germany) palatal miniscrews were inserted into the anterior maxilla to anchor HH appliance (Figure 1) [19]. Under local anaesthesia, mucoperiosteal flap was elevated and Mentoplates (ANCOR Orthodontics, Ankara, Türkiye) were fixed to the anterior symphysis with three screws. HH appliance was activated twice daily (0.5 mm/day) for 7 days, achieving 3.5 mm expansion prior to protraction. After RPE, full-time Class III elastics (200–250 g per side) were applied between HH molar band and Mentoplate hooks. Patients were reviewed every 6 weeks to adjust force levels and monitor skeletal units. Active treatment ended after at least a half-cusp canine relationship improvement, and final records were obtained immediately (Figure 1). No fixed orthodontic appliances were used during maxillary protraction phase. Mean interval between initial and final CBCTs corresponded to treatment duration (12.62 ± 1.7 months, minimum: 10.4; maximum: 15.6, Table 1).

2.5 | Variables

Primary outcomes were defined as sagittal skeletal changes (SNA, ANB), vertical skeletal changes (SN-MP, N-Me), and

TABLE 1 | Descriptive statistics of study group and definition of the landmarks, lines and measurements.

Statistics of study group		
Initial age (years)	11.7 ± 1.32	
Female	12.08 ± 1.43	
Male	10.86 ± 1.05	
Treatment duration (months)	12.62 ± 1.7	
Stage of maturational growth		
CS2	6	
CS3	6	
CS4	5	

	T0	
	Mean	SD
SNA	79.91	3.13
SNB	80.3	3.00
ANB	−0.22	2.06
AFH	111.61	3.19
PFH	68.74	2.61
Jarabak ratio (PFH/AFH × 100)	61.6	1.85
SN-GoMe	40.55	1.75

Abbreviations	Definition
S	Geometric center of Sella turcica
N	The most anterior point of the frontonasal suture in midsagittal plane
A	The most posterior point of the concavity of the anterior segment of the maxilla
B	The most posterior point of the concavity of the anterior segment of the mandible
ANS	The tip of the anterior nasal spine of the maxilla in the midsagittal plane
PNS	The most posterior point of the hard palate in the midsagittal plane
Pog	The most anterior point of the symphysis
Gn	Midpoint of the curvature of the pogonion and menton
Me	The most inferior point of the symphysis
RPo, LPo	The most superior point of the roof of the right and left external auditory meatus
Po_m	The 3D centre point calculated as the average of the X, Y and Z coordinates of the RPo and LPo
ROr, LOr	The lowest point on the lower part of the right and left orbital contour

(Continues)

TABLE 1 | (Continued)

Abbreviations	Definition
Or_m	The 3D centre point calculated as the average of the X, Y and Z coordinates of the ROr and LOr
RNC, LNC	The most inferior and exterior point of the concavity of the right and left nasal cavity
NC_m	The 3D centre point calculated as the average of the X, Y and Z coordinates of the RNC and LNC
RZyg, LZyg	The most inferior portion of the right and left zygomatic bones
Zyg_m	The 3D centre point calculated as the average of the X, Y and Z coordinates of the RZyg and LZyg
RJ, LJ	The junction of the zygomatic buttress and maxilla tuberosity at both sides
J_m	The 3D centre point calculated as the average of the X, Y and Z coordinates of the RJ and LJ
RGo, LGo	The projection of a virtual bisector of a line adjacent to the posterior side of mandibular ramus and corpus on both sides
Go_m	The 3D centre point calculated as the average of the X, Y and Z coordinates of the RGo and LGo
RCo, LCo	The most superior and central point of both condyles
Co_m	The 3D centre point calculated as the average of the X, Y and Z coordinates of the RCo and LCo
Mx1	Incisal midpoint of maxillary right central
Mnd1	Incisal midpoint of mandibular right central
11a	Apex of maxillary right central
41a	Apex of mandibular right central
16mb, 26mb, 36mb, 46mb	Mesio-buccal cusp tips of first permanent molars
UM	The 3D centre point calculated as the average of the X, Y and Z coordinates of 16mb and 26mb
LM	The 3D centre point calculated as the average of the X, Y and Z coordinates of 36mb and 46mb
FH	The line passing through the Po_m and Or_m

(Continues)

TABLE 1 | (Continued)

Abbreviations	Definition
OP	The line passing through the midpoint of UM and LM, and the midpoint of Mx1 and Mnd1
PP	The line passing through ANS and PNS
MP	The line passing through Go_m and Me
SN	The line passing through S and N
UI	The line passing through Mx1 and 11a
LI	The line passing through Mnd1 and 41a
UM-PP	Superoinferior component of the perpendicular distance of the UM point to the PP
LM-MP	Superoinferior component of the perpendicular distance of the LM point to the MP
OJ	Anteroposterior component of the distance between Mx1 and Mnd1
OB	Superoinferior component of the distance between Mx1 and Mnd1
N′	Deepest point of the nasal bridge angle
Sn′	Median point at the junction between the lower border of the nasal septum and the philtrum area
AlR′, AlL′	Outermost point of the alar contours on both sides
Ls′	Midpoint of the vermilion line of the upper lip
Li′	Midpoint of the vermilion line of the lower lip vermilion
PFH	Posterior facial height: The superoinferior component of the distance between S and midpoint of RGo and LGo
AFH	Anterior facial height: The superoinferior component of the distance between N and Me
SS (Sphenoid Sinus) Plane	Horizontal plane parallel to the FH plane, intersecting the inferior part of the floor of the sphenoid sinus
PNS-H Plane	Horizontal plane parallel to the FH, passing through PNS
PNS-F Plane	Frontal plane perpendicular to FH, passing through PNS
U Plane	Horizontal plane parallel to the FH, passing through the inferior portion of the uvula

(Continues)

TABLE 1 | (Continued)

Abbreviations	Definition
E Plane	Horizontal plane parallel to the FH, passing through the superior portion of the epiglottis
C2P (Second cervical vertebra) Plane	Frontal plane perpendicular to FH, passing through the posterior part of the second cervical vertebra
MS Plane (Maxillary Sinus Plane)	Passing through the external walls of each maxillary sinus, this completely vertical relative to the FH.

Abbreviation: SD, standard deviation.

airway volumes (Nasopharynx (NPh), Middle Pharynx (MPh)). All other variables were considered secondary outcomes.

2.6 | Data Sources and Measurement

Entire digital workflow was performed by a single investigator (G.Y.). During CBCT acquisition (Iluma Imtec Imaging Machine device; 3M, Ardmore, OK, USA; X-ray tube voltage: 120 kV; X-ray tube current: 1–4 mA; scanning time: 40 s with 360° rotation; field of view: 14.2×21.1 cm; voxel size: 0.0936 mm; grey scale: 14 bit), patients' Frankfort horizontal plane (FH) was parallel to the floor, and they were sitting upright. Additionally, to assure a correct and reproducible bite, all patients were instructed to occlude in maximum intercuspation using a silicone bite registration material. Images were taken in 'Digital Imaging and Communications in Medicine' (DICOM) format. In our clinic routine pre- and post-treatment CBCT imaging, strictly adhering to ALARA (As Low As Reasonably Achievable) principles, is utilized to ensure precise insertion and minimally invasive removal of miniscrews and Mentoplates to preserve bone and soft tissue.

3D Slicer 5.8.1 program was used to segment the DICOM data and perform the analysis [20]. All DICOM images were reoriented by aligning midsagittal, FH and transporionic planes with sagittal, axial and coronal planes, respectively [21]. Artificial intelligence-based automatic cranial base segmentation was carried out using Slicer Automated Dental Tools extension, AMASSS module [22, 23]. Subsequently, manual refinement was performed using 'Segment Editor' tool. Any over-segmentation or under-segmentation artefacts were corrected manually slice-by-slice without applying a standardized automated thresholding value. Voxel-based registration method was carried out to superimpose T1 image over oriented T0 image using cranial base as a reference (Figure 2). Maxilla, mandible, airway and skin were segmented using AMASSS module, and 3D models were created [23]. Predetermined landmarks were placed on models and checked via T0 and T1 DICOM images (Table 1, Figure 3). Standardized airway dimensions were calculated using specific anatomical reference planes, while Sphenoid Sinus (SS) Plane served as the most superior border, Epiglottis (E) Plane was the most inferior limit. Posterior Nasal Spine-Frontal (PNS-F) Plane provided the anterior boundary, Second Cervical Vertebra (C2P) Plane defined the posterior limit, and Maxillary Sinus (MS)

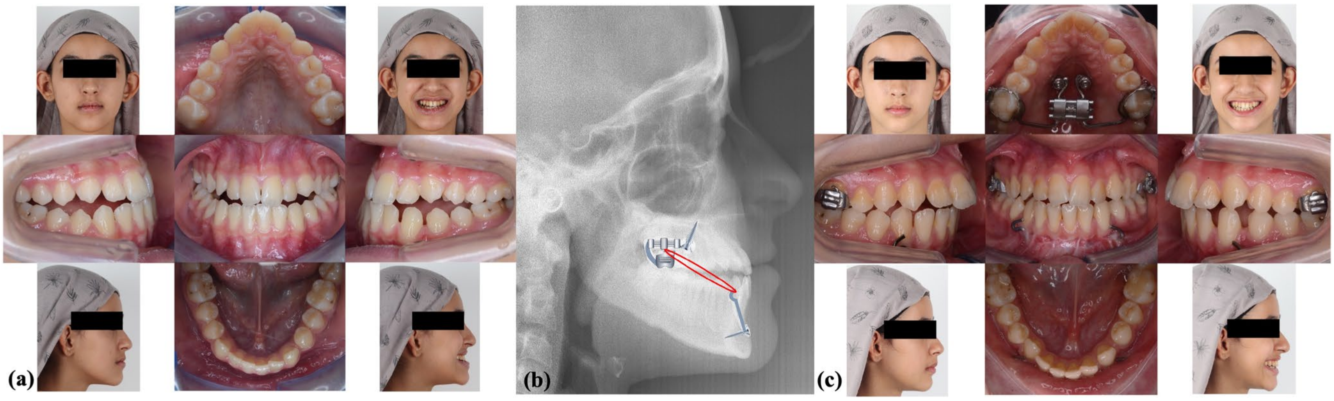

FIGURE 1 | Representative case of the study group. The patient's starting age was 12 years and 1 month, with a CVM stage of 3 at the outset of treatment. The total treatment duration (T0–T1) was 11 months and 21 days. This patient reflects the typical skeletal and dental characteristics of the overall study population. (a) Initial extraoral and intraoral records. (b) Schematic illustration of the hybrid hyrax-mentoplate appliance configuration. (c) Final extraoral and intraoral records.

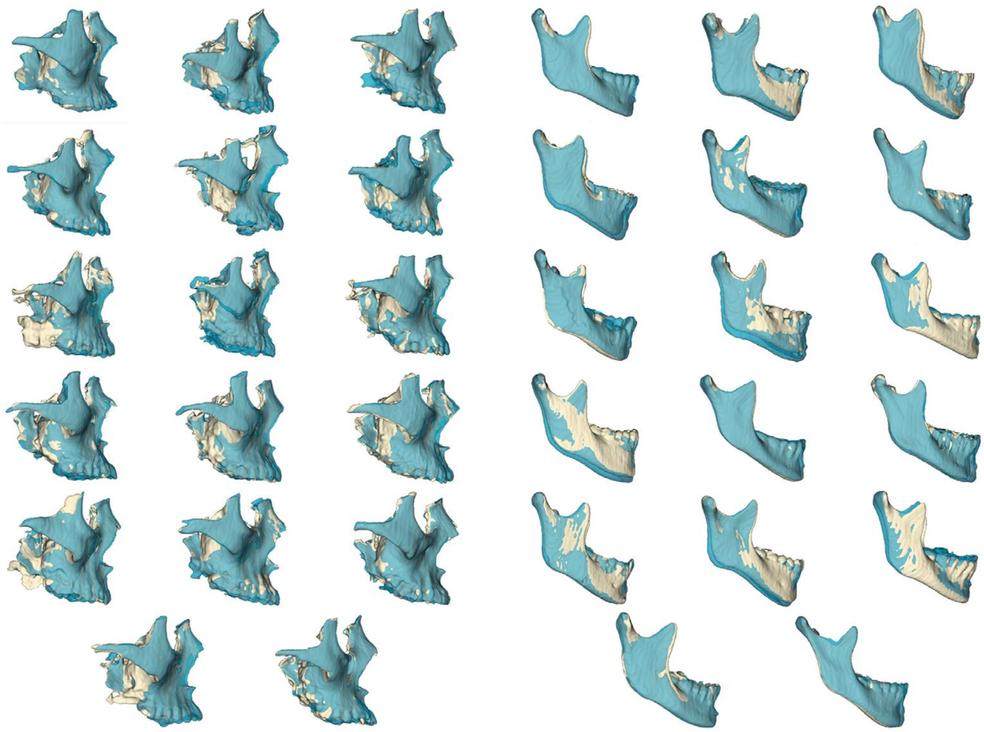

FIGURE 2 | Superimposed T0 and T1 maxilla and mandible models of all individuals included in the study, with reference to the cranial base.

Plane established the lateral boundaries (Table 1, Figure 3). Total airway was also divided into sub-segments: NPh was defined between SS and PNS-Horizontal (PNS-H) Planes, MPh was between PNS-H and Uvula (U) Planes, and inferior pharynx (IPh) extended between U and E Planes (Table 1, Figure 3) [14]. 3D volume measurements were made in cubic millimetres (mm^3) using 'Segment Statistics' in the software.

Q3DC module was used to generate midpoints (e.g., Go_m: 3D centre point calculated as average of X, Y and Z coordinates of both Gonions) and calculated angular, linear, and 3D displacements. To facilitate clinical interpretation, the 3D coordinates of the anatomical landmarks were projected onto the sagittal, vertical and transverse planes. This allowed for the calculation of standard angular and linear measurements, ensuring that the results remain comparable with existing literature. Landmark changes ($\Delta T1-T0$) were measured anteroposteriorly, superoinferiorly and as total 3D displacements (Table 2). Positive values denote anterior and superior movements, whereas negative values indicate posterior and inferior displacements (Table 2). All angles represent pitch rotations between the specified landmarks or reference lines (Table 3).

2.7 | Bias

It is acknowledged that restricting the study group exclusively to fully compliant patients inherently introduces a selection

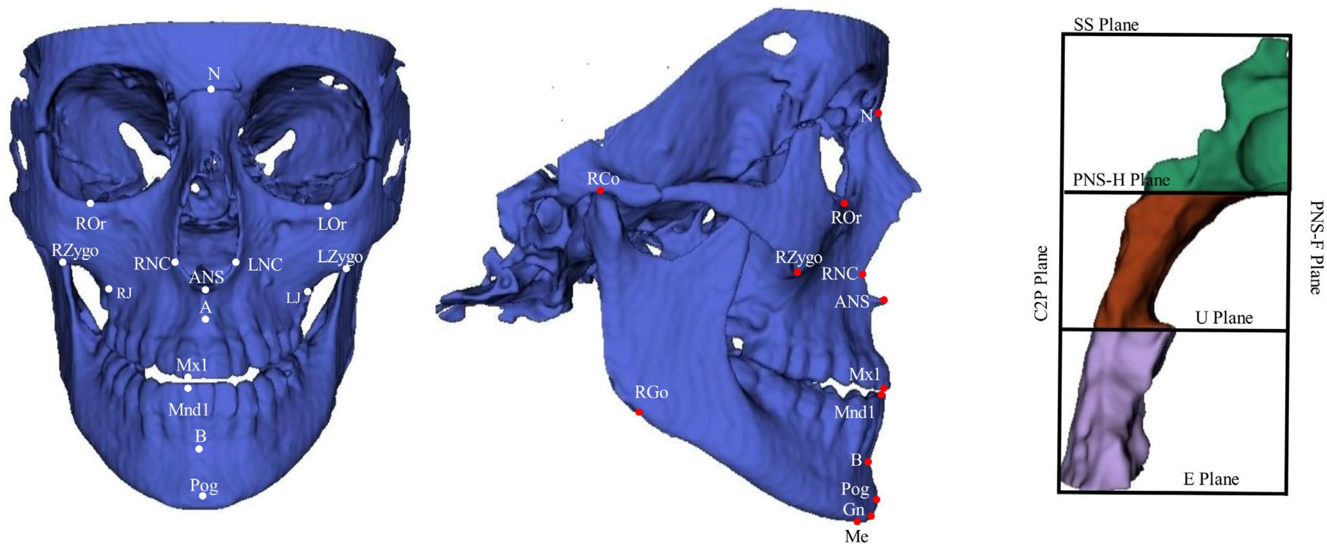

FIGURE 3 | Some reference points and planes used in the study.

bias, as it excludes those who failed to complete the protocol. However, to mitigate other potential confounding factors, uniform eligibility criteria were strictly applied. Measurement bias was minimized by acquiring all data on a single CBCT device and a standardized segmentation/registration workflow.

2.8 | Statistical Analysis

Statistical analysis was done using IBM SPSS Statistics (version 23, IBM Corp, Armonk, NY) software. All variables of 30% of randomly selected patients were measured again after 1 month to assess intra-examiner reproducibility and calculate intraclass correlation coefficient (ICC).

Shapiro–Wilk test was implemented to assess the normality of variables. Normally distributed variables were analysed with paired-sample *t*-test and treatment changes over time ($\Delta T1 - T0$) were reported as mean difference along with its 95% CI. Conversely, non-normally distributed variables were evaluated using Wilcoxon signed-rank test and treatment changes were reported as Hodges–Lehmann point estimate of median difference, accompanied by the corresponding Hodges–Lehmann 95% CI. $p < 0.05$ was considered statistically significant. However, to address the potential inflation of Type I error from multiple testing, we predefined a focused set of primary outcomes (SNA, ANB, SN-MP, N-Me, NPh and MPh) directly related to our primary hypotheses. All other measurements were considered exploratory secondary outcomes and their *p*-values are reported without multiple comparison adjustments.

3 | Results

ICC varied between 0.857 and 0.998, indicating good to excellent intra-examiner reliability. No missing data were observed for any variable at T0 or T1; therefore, all analyses were conducted on complete dataset. All following outcomes reflect a study group that completed the treatment with full compliance. Cephalometric values and Cervical Vertebral Maturation stages of the study group at T0 are given in Table 1. The first hypothesis was accepted as the facial height is not affected. However, the second hypothesis was accepted for NPh and MPh regions, as significant volumetric increases were detected in these segments, but rejected for IPh.

Antero-posterior, supero-inferior and 3D distance changes of certain landmarks are given in Table 2.

3.1 | Main Results

Regarding primary outcomes, statistically significant increases were found in SNA ($p < 0.001$, Cohen's $d = 2.04$) and ANB angles ($p < 0.001$, Cohen's $d = 1.73$) (Table 3). No significant changes were found in SN-MP angle and N-Me (Table 3). For airway, significant increases were detected in NPh ($p = 0.008$, Cohen's $d = 0.74$) and MPh volumes ($p = 0.003$, Cohen's $d = 0.83$) (Table 3).

In sagittal evaluation, significant increases were detected in Co_m-Gn, Co_m-A, Go_m-Gn measurements ($p = 0.002$, $p < 0.001$, $p = 0.001$, Table 3, respectively).

In vertical examination, a significant increase was observed in occlusal plane (OP) to MP angle ($p = 0.001$, Table 3), and statistically significant decreases were found in SN-OP and palatal plane (PP) to OP angles ($p = 0.008$, $p = 0.008$, respectively, Table 3). In vertical soft tissue measurements, a significant increase was noted in soft tissue nasion to lower lip (N′-Li′) ($p = 0.003$, Table 3).

In transverse measurements, significant increases were observed in mesio-buccal cusps of upper first molars (16mb-26mb), right and left jugale (RJ-LJ), right and left zygomatic bones (RZygo-LZygo), right and left nasal cavity (RNC-LNC), right and left alare (AlR′-AlL′) ($p = 0.002$, $p = 0.011$, $p < 0.001$, $p < 0.001$, $p = 0.001$, respectively, Table 3).

Dental evaluation showed statistically significant increases in upper molar (UM) to PP, upper incisor (UI) to PP, lower incisor

TABLE 2 | Descriptive statistics of 3D displacements.

	Anteroposterior displacement (mm)			
	Mean ± SD	**Median**	**Min**	**Max**
A	2.65 ± 1.21	2.59	0.59	5.30
B	0.55 ± 2.03	0.18	−1.74	3.91
ANS	2.02 ± 1.07	2.27	0.07	3.80
Me	0.23 ± 2.10	0.11	−3.37	3.97
Gn	0.23 ± 2.35	0.09	−3.64	3.86
Pog	0.52 ± 2.08	0.12	−2.18	3.22
J_m	2.37 ± 1.48	2.24	−0.09	4.55
Zyg_m	1.52 ± 0.93	1.37	−0.19	3.24
Mx1	4.39 ± 1.93	4.15	1.03	6.98
Or_m	0.80 ± 0.72	0.88	−0.43	1.82
NC_m	1.61 ± 1.23	1.51	−0.15	4.40
Co_m	−0.27 ± 0.90	−0.24	−2.35	1.09
Go_m	−0.98 ± 1.74	−1.25	−3.49	2.84
Sn′	2.27 ± 1.44	1.89	0.28	4.94
Ls′	2.80 ± 1.80	2.14	0.66	6.56
Li′	0.99 ± 1.89	1.08	−2.03	4.09
	Superoinferior displacement (mm)			
	Mean ± SD	**Median**	**Min**	**Max**
A	−1.22 ± 1.92	−1.81	−4.43	2.15
B	0.76 ± 3.44	0.88	−5.38	5.65
ANS	−0.73 ± 1.27	−0.42	−4.89	0.40
Me	−1.04 ± 2.35	−1.34	−4.23	3.09
Gn	−1.14 ± 2.00	−1.01	−3.84	3.23
Pog	−0.36 ± 2.09	−0.37	−3.59	3.50
J_m	−1.20 ± 1.22	−1.19	−3.45	0.69
Zyg_m	−0.38 ± 0.95	−0.52	−3.07	0.84
Mx1	−1.10 ± 1.51	−1.01	−6.00	0.88
Or_m	−0.06 ± 0.58	−0.01	−1.44	1.00
NC_m	−0.22 ± 1.08	−0.29	−1.93	1.82
Co_m	0.25 ± 0.79	0.11	−1.11	2.61
Go_m	−0.48 ± 1.81	−0.22	−5.13	3.08
Sn′	−0.28 ± 1.56	0.05	−4.81	1.78
Ls′	−0.43 ± 1.43	0.04	−3.46	0.95
Li′	−1.77 ± 2.11	−1.51	−5.52	1.66
	3D displacement (mm)			
	Mean ± SD	**Median**	**Min**	**Max**
A	3.57 ± 1.00	3.63	1.47	5.32

(Continues)

TABLE 2 | (Continued)

	3D displacement (mm)			
	Mean ± SD	**Median**	**Min**	**Max**
B	3.81 ± 1.48	3.65	1.53	6.49
ANS	2.52 ± 1.12	2.62	0.80	5.34
Me	3.10 ± 1.34	2.96	0.57	4.76
Gn	3.13 ± 1.22	3.06	0.70	5.00
Pog	2.89 ± 1.02	3.22	0.73	4.66
J_m	3.14 ± 1.36	3.12	0.81	4.96
Zyg_m	1.94 ± 0.91	2.00	0.57	3.71
Mx1	4.68 ± 1.96	4.53	1.60	9.24
Or_m	1.38 ± 0.51	1.48	0.48	2.33
NC_m	2.04 ± 1.08	1.95	0.44	4.44
Co_m	1.24 ± 0.63	1.05	0.65	2.88
Go_m	2.52 ± 1.27	2.50	0.76	5.82
Sn′	2.75 ± 1.55	2.42	1.03	6.25
Ls′	3.30 ± 1.63	3.03	1.47	6.63
Li′	3.08 ± 1.53	2.67	1.42	6.22

Note: positive (+) values for anterior and superior displacements; negative (−) values for posterior and inferior displacements.
Abbreviations: m; midpoint; max; maximum; min; minimum; SD; standard deviation.

(LI) to MP, and overjet ($p < 0.001$, $p = 0.018$, $p = 0.048$, $p < 0.001$, respectively, Table 3).

4 | Discussion

It is known that conventional FM applies clockwise rotation to the mandible and increases facial height [24]. However, Pavoni et al. [25] demonstrated that a 30° downward and forward FM protraction force produced minimal vertical skeletal changes, regardless of the patient's vertical pattern. Likewise, incorporating a bite-block improves vertical control [26]. While specific biomechanical adjustments can mitigate vertical side effects, traditional FMs remain limited by a restricted optimal age range and poor patient compliance due to their extraoral design [3, 10]. By utilizing fully intraoral components, HH-M protocol eliminates tooth-borne side effects and improves patient acceptance. This approach enables effective orthopaedic correction even in older age groups or patients unable to tolerate FM [6, 27, 28].

The literature describes various skeletal anchorage techniques that successfully maintain vertical height [1, 3, 9–11, 16, 27–30]. Protocols utilizing miniplates with FM support on lateral nasal or anterior maxillary walls report no vertical increases [11, 29]. Bone-Anchored Maxillary Protraction (BAMP) approach also induces minimal vertical alterations, providing a viable option for high-angle individuals [10, 30]. When HH is used as maxillary anchorage, overbite remains stable during FM therapy [27, 28]. Specific to HH-M approach, the absence of vertical

TABLE 3 | Treatment changes of study group over time.

	T0	T1	ΔT1 – T0	95% CI	*p*
Primary outcomes					
SNA (°)[a]	79.91 ± 3.13	82.42 ± 3.05	2.51 ± 1.23	1.88 to 3.14	< 0.001***
ANB (°)[a]	−0.22 ± 2.06	1.91 ± 1.48	2.13 ± 1.23	1.50 to 2.76	< 0.001***
SN-MP (°)[b]	39.65 (39.21, 41.10)	40.51 (38.46, 41.15)	−0.50	−1.23 to 0.25	0.227
N-Me (mm, SI)[a]	111.61 ± 3.19	112.45 ± 4.12	0.85 ± 2.21	−0.29 to 1.98	0.134
Nasopharynx (mm^3)[a]	3676.77 ± 1358.27	4263.22 ± 1315.60	586.45 ± 792.39	179.02 to 993.88	0.008**
Middle pharynx (mm^3)[a]	5024.57 ± 1877.67	6041.43 ± 1753.33	1016.86 ± 1224.71	387.15 to 1646.58	0.003**
Secondary outcomes					
Sagittal					
SNB (°)[a]	80.30 ± 3.00	80.52 ± 3.11	0.22 ± 1.24	−0.42 to 0.86	0.475
Co_m-Gn (mm, 3D)[a]	107.29 ± 5.48	109.04 ± 5.59	1.75 ± 1.94	0.75 to 2.75	0.002**
Co_m-A (mm, 3D)[a]	75.98 ± 3.99	79.34 ± 3.64	3.36 ± 1.33	2.68 to 4.05	< 0.001***
Go_m-Gn (mm, 3D)[a]	67.06 ± 3.65	68.83 ± 3.88	1.77 ± 1.78	0.85 to 2.69	0.001**
Vertical					
SN-PP (°)[a]	9.67 ± 2.77	8.76 ± 3.02	−0.90 ± 2.05	−1.96 to 0.15	0.088
PP-MP (°)[a]	29.93 ± 3.15	30.36 ± 3.40	0.42 ± 2.30	−0.76 to 1.60	0.461
SN-OP (°)[a]	18.88 ± 3.15	16.68 ± 3.97	−2.20 ± 3.01	−3.75 to −0.66	0.008**
PP-OP (°)[a]	9.21 ± 3.13	7.08 ± 3.95	−2.13 ± 2.89	−3.62 to −0.65	0.008**
OP-MP (°)[a]	20.72 ± 2.50	23.39 ± 3.77	2.67 ± 2.63	1.32 to 4.02	0.001**
Co_mGo_mMe (°)[a]	132.13 ± 5.04	131.36 ± 5.12	−0.78 ± 3.06	−2.35 to 0.80	0.311
N-ANS (mm, SI)[b]	50.40 (49.18, 50.98)	50.81 (49.52, 51.52)	0.45	−0.03 to 0.94	0.093
ANS-Me (mm, SI)[b]	60.58 (59.73, 63.95)	61.01 (57.82, 62.66)	0.12	−1.12 to 1.22	0.793
Co_m-Go_m (mm, 3D)[a]	51.28 ± 2.42	52.17 ± 2.83	0.89 ± 1.56	0.09 to 1.70	0.032*
N′-Sn′ (mm, SI)[b]	47.00 (45.59, 47.98)	47.07 (45.82, 47.33)	−0.03	−0.69 to 0.71	0.408
N′-Ls′ (mm, SI)[b]	58.01 (57.15, 61.50)	59.85 (57.46, 61.40)	0.23	−0.35 to 1.25	0.201
N′-Li′ (mm, SI)[a]	73.86 ± 3.62	75.63 ± 2.51	1.77 ± 2.11	0.68 to 2.85	0.003**
Transverse					
16mb-26mb (mm, 3D)[b]	51.75 (48.88, 53.37)	52.76 (51.56, 54.07)	2.28	1.04 to 3.44	0.002**
RJ-LJ (mm, 3D)[a]	61.01 ± 3.54	62.53 ± 3.66	1.52 ± 2.19	0.40 to 2.64	0.011*
RZygo-LZygo (mm, 3D)[a]	82.64 ± 4.30	84.70 ± 3.74	2.06 ± 1.75	1.16 to 2.96	< 0.001***
RNC-LNC (mm, 3D)[a]	19.73 ± 1.85	21.98 ± 1.88	2.25 ± 1.01	1.73 to 2.77	< 0.001***
AlR′-AlL′ (mm, 3D)[a]	31.19 ± 2.15	32.53 ± 2.27	1.34 ± 1.28	0.68 to 2.00	0.001**

(Continues)

	T0	T1	ΔT1 − T0	95% CI	p
Dental					
UI-PP (°)[a]	113.08 ± 7.67	116.03 ± 6.32	2.95 ± 4.59	0.58 to 5.31	0.018*
LI-MP (°)[a]	82.02 ± 4.83	84.22 ± 4.19	2.20 ± 4.24	0.02 to 4.38	0.048*
UM-PP (mm, SI)[a]	20.39 ± 2.23	22.04 ± 2.96	1.64 ± 1.40	0.92 to 2.36	< 0.001***
LM-MP (mm, SI)[a]	22.40 ± 2.71	22.24 ± 3.30	−0.17 ± 1.16	−0.76 to 0.43	0.562
OJ (mm)[b]	−1.43 (−2.33, −0.06)	2.22 (1.94, 2.46)	3.60	2.76 to 4.33	< 0.001***
OB (mm)[a]	−0.61 ± 1.82	0.49 ± 1.61	1.10 ± 2.31	−0.09 to 2.29	0.067
Airway					
Inferior pharynx (mm^3)[a]	2319.31 ± 873.58	2373.01 ± 876.81	53.71 ± 897.97	−408.01 to 515.42	0.808

Note: Values for T0 and T1 are reported as Mean ± SD for the paired-sample *t*-test and as Median (Interquartile Range) for the Wilcoxon signed-rank test. For the Wilcoxon signed-rank test, the ΔT1 − T0 column displays the Hodges–Lehmann (HL) point estimate of the median difference. The 95% CI column represents the 95% confidence interval of either the mean difference (paired-sample *t*-test) or the HL estimate (Wilcoxon signed-rank test).
Abbreviations: 3D, three-dimensional distance; CI, confidence interval; m, midpoint; mm, millimetres; mm^3, cubic millimetres; SD, standard deviation; SI, superoinferior component.
[a]Paired-sample *t*-test.
[b]Wilcoxon signed-rank test.
*$p < 0.05$.
**$p < 0.01$.
***$p < 0.001$.

changes confirms its suitability for high-angle patients [3, 9, 16]. Meyns et al. [1] applied Alternate Rapid Maxillary Expansion and Constriction protocol with HH-M and did not observe any change in MP angle.

All the aforementioned investigations evaluated patients with normal or decreased vertical patterns [1, 3, 9, 16, 19, 31]. To our knowledge, no existing literature examines the outcomes of high-angle patients receiving HH-M therapy. Only one study applied Class III orthopaedic treatment to a high-angle cohort; however, their expansion protocol differed from ours [31]. Therefore, this study is the first to investigate the HH-M approach not only with traditional linear and angular measurements but also with total 3D displacements and volume changes in high-angle patients.

In this study, voxel-based superimposition was performed using cranial base as reference in CBCT images, a method previously validated for its accuracy and reproducibility in growing subjects [32, 33]. Validated AI-based instruments were also used to segment the mandible, maxilla, and cranial base using 3D Slicer software, AMASSS module [22, 23].

Similar to prior studies, significant alterations were noted in SNA and ANB angles, although no variation was detected in SNB angle [3, 9, 16]. Minor variations from previous studies are likely due to their 2D imaging, alongside variations in sample age and vertical patterns. Increased movement in antero-posterior direction at point A relative to point B corroborates this finding (A: 2.65 ± 1.21, B: 0.55 ± 2.03). Moreover, Co_m-A is increased significantly, which indicates anterior movement of maxilla. In the literature, a 1.4° increase in the SNA angle and a 2 mm increase in Co-A have been reported to be clinically significant [34, 35]. In light of this information, it can be speculated that the findings of this study are clinically significant (ΔT1 − T0 SNA: 2.51 ± 1.23; ΔT1 − T0 CoA: 3.36 ± 1.33). Go_m-Gn and Co_m-Go_m also significantly increased, indicating that both sagittal and vertical growth occurred, which explains the increase in Co_m-Gn. However, the clinically significant threshold value for Co_m-Gn has been reported as 2 mm in the literature, so the significant increase in Co_m-Gn might be clinically negligible (ΔT1 − T0 Co_m-Gn: 1.75 ± 1.94) in this study [36]. The lack of a control group prevents distinguishing between natural growth and treatment-suppressed growth. In the study by Miranda et al. [37] comparing the MAMP and BAMP protocols, antero-posterior displacement of point A in our study was less than BAMP protocol, but greater than MAMP group. Miranda et al. [37] indicated in their study that the BAMP treatment may exhibit slightly higher efficacy in maxillary advancement. In supero-inferior direction, more inferior movement at A was observed in this study compared to both techniques [37]. Facio-Umaña et al. [31] applied skeletally anchored Class III orthopaedic treatment to a high-angle cohort, utilizing an aggressive expansion protocol (two turns per day for 2 weeks, then one turn per day) by four miniscrews and bilateral mandibular miniplates applying 100–200 g per side for an average of 4.46 months. Despite our heavier elastic forces and longer treatment duration, they observed greater increases in SNA and ANB angles. This difference can be attributed to a more extensive sutural disarticulation due to aggressive expansion protocol. In another study, Ngan et al. [6] evaluated the effects of maxillary protraction using HH-FM. Although the maxillary anchorage unit was identical, a greater increase in SNA angle was demonstrated in this study, which might be due to extended treatment duration, despite their younger cohort and heavier orthopaedic forces. Moreover, Liang et al. [29] used patient-specific customized miniplates with FM and found significant increase in the SNA angle consistent with our findings.

No significant change was found in SN-PP, SN-MP, PP-MP angles, N-Me, N-ANS, ANS-Me indicating that vertical skeletal dimensions were preserved during treatment. The downward movement of Go_m and Me points in supero-inferior direction by 0.48 and 1.04 mm, respectively, suggests that mandibular plane remains almost parallel to its initial location, corroborating the observation of no alteration in SN-MP angle. Most of the studies also observed no alterations in angular measurements, especially in SN-MP angle, consistent with our findings [3, 9, 31]. In light of current literature, the preservation of vertical dimension can be strongly attributed to the synergistic biomechanical advantages of both HH and Mentoplate [1, 9, 38]. First, by utilizing miniscrews in maxilla, HH ensures that the expansion and protraction forces are delivered closer to the centre of resistance of maxilla. Second, Mentoplate provides a stable, bony intraoral point, and anchoring elastics directly to Mentoplate, the force vector is reduced to an angle of approximately 10°–15° relative to OP [9]. Consequently, it is hypothesized that this more horizontal vector might neutralize the counterclockwise rotational moment, which could theoretically facilitate a more translational advancement of maxilla and prevent unwanted vertical opening. Consistent with the present investigation, Ngan et al. [6] reported no significant changes in mandibular plane angle. However, it is important to note that their study evaluated a normodivergent cohort. Liang et al. [29] also observed no significant changes in SN-MP using customized maxillary miniplates, which is in accordance with our results. Conversely, Katyal et al. [16] noted a substantial reduction in SN-PP angle, though they considered it clinically insignificant. Tarraf et al. [3] and Katyal et al. [16] also reported no significant change in overbite as our study. Moreover, Co_mGo_mMe (gonial) angle is preserved during treatment, similar to previous 2D studies [3, 16]. The decrease in gonial angle in our study was very similar to MAMP group of Miranda et al. [37], but less than their BAMP group. Conversely, Willman et al. [9] reported a significant decrease in gonial angle different than this study, which is likely due to their sample of vertically normal-low angle individuals.

Compared to Miranda et al. [37], the Go_m point in this study moved more posteriorly than in their MAMP group but less than in their BAMP group [37]. Therefore, while all three modalities displace gonial region posteriorly, the HH-M approach appears to be more effective in maintaining vertical position of Go point. Similarly, the Pog point exhibited less anterior and inferior displacement [37], suggesting that the HH-M technique may better preserve the overall spatial position of the chin.

Anterior chin landmarks (B′ and Pog′) were excluded from the soft tissue evaluation due to physical distortion by Mentoplate. Vertical soft tissue measurements remained unchanged except for N′–Li′ distance, which is likely due to the 1.77 mm inferior displacement of lower lip caused by the appliance.

Changes in SN-OP, PP-OP and OP-MP angles indicated a counterclockwise rotation of OP. This rotation is further supported by significant UM extrusion observed, while lower molars remained vertically stable. Although HH-M technique aims to keep the elastic vector as horizontal as possible, the inherently steeper vector in high-angle individuals compared to normal-low angle subjects may have contributed to this outcome. Although UM extrusion has been reported with this technique similar to ours [18], other studies likely missed this side effect because they lacked vertical molar assessments, relied on 2D imaging, and focused on normal-to-low angle individuals [3, 9, 16].

Some of the studies found no changes in lower incisor angle [9, 16]; however, this study noted significant proclination, which is consistent with the findings of Tarraf et al. [3]. This can be explained by the lip bumper effect of Mentoplate hooks, as proposed previously [11]. Furthermore, contrary to previous HH-M reports [3, 9, 16], notable upper incisor proclination was also detected. This is likely a dental side effect of anchoring HH appliance to dentition via molar bands [18, 35, 37]. Moreover, despite bimaxillary incisor proclination, overjet improvement may be primarily attributed to true skeletal maxillary protraction, which is confirmed by 3D displacement data, where maxillary reference points (A, ANS, J_m, $Zygo_m$ and NC_m) moved more forward relative to mandibular landmarks (Me, Gn and Pog).

Significant increase was observed in all transverse measurements and can be attributed to the effect of applied RPE. Parallel with the literature, an increase in distance of alar wings was noted alongside the skeletal increase of nasal level [39].

This study revealed an increase in volume of NPh and MPh, whereas no change was found in IPh. Although the utilization of different anatomical airway boundaries in between studies, increases in airway volume similar to our study have been reported in skeletal anchorage-supported Class III treatments [12, 13]. In the study of Steegman et al. [14] although the same anatomical boundaries were used, significant increases were found only for NPh and total airway volume. Difference for MPh might be due to their cleft lip and palate patients. However, clinical significance of these volumetric changes still remains unclear. Although an increase in airway volume may theoretically improve airflow, it may not necessarily create functional improvements such as reduced respiratory symptoms or improved sleep-related breathing problems. A systematic review has highlighted that the current evidence regarding airway enlargement following BAMP is limited and heterogeneous, and the magnitude of volumetric change may not reach a clinically meaningful threshold [15]. Moreover, although Steegman et al. [14] reported significant airway volume increase following BAMP protocol, results were comparable to untreated Class III control group which may also raise questions regarding clinical relevance of the findings.

On the other hand, Katyal et al. [16] did not see a linear alteration in adenoid level in their HH-M approach. Yet the variation in approaches utilized and 2D examinations may be the reason for these differences.

Another important consideration is the relationship between skeletal correction and airway changes. In a randomized clinical trial evaluating MAMP, although significant increases in oropharyngeal volume were observed, no significant correlation was detected between skeletal changes and airway modifications [12]. This suggests that airway adaptations may not depend truly on skeletal changes but also on complex interactions between surrounding soft tissues and neuromuscular adaptation.

CBCT measurements are naturally sensitive to instantaneous factors like head posture, tongue position, or breathing phase during the scan. Thus, volumetric increases we observed in NPh and MPh regions should be interpreted with caution. Furthermore, even though we noted a clear transverse expansion at skeletal nasal region, we did not specifically segment the internal nasal cavity to quantify its volume changes [39]. Adding functional respiratory tests and internal nasal evaluations in future trials would provide a clearer picture of breathing effects with treatment.

While HH-M technique offers clear orthopaedic benefits, its clinical challenges and higher costs compared to conventional methods must be considered. Unlike traditional FM, this protocol requires two separate surgical interventions to place and remove the Mentoplates. Our initial screenings revealed complications including soft tissue irritation, one instance of inflammatory fibrous hyperplasia, and one necessary plate repositioning surgery. These clinical hurdles, coupled with rigorous demand for full-time Class III elastic wear, led to the exclusion of four patients due to non-compliance. Therefore, clinicians should be aware that this approach demands highly motivated patients to overcome the surgical burden and potential side effects. Reported outcomes reflect the efficacy of the protocol under conditions of full compliance.

4.1 | Limitations and Generalisability

Our study has certain limitations that should be kept in mind. Most importantly, without an untreated high-angle control group, it is difficult to precisely differentiate the true orthopaedic effect from natural growth and skeletal maturation. The single-arm design and slight variations in individual active treatment durations (SD: 1.7 months) might also introduce minor confounding effects. Additionally, we currently lack long-term follow-up records to evaluate the stability of these orthopaedic corrections over time.

Finally, since all 3D digital workflows were completed by a single examiner in a single centre, inter-examiner reproducibility was not assessed, and the results might not be fully generalizable. Findings should be extrapolated only to growing Class III patients presenting similar age and dentoskeletal profiles who demonstrate full compliance with the treatment protocol. Future multicentre studies with larger sample sizes comparing HH-M protocol to other high-angle Class III interventions are recommended.

5 | Conclusion

This study provides the first 3D evidence that, in fully compliant patients who successfully complete the protocol, the HH-M technique effectively achieves maxillary protraction while successfully maintaining vertical skeletal stability even in high-angle subjects, highlighting the incremental value of this approach. Additionally, the protocol induces transverse expansion in the maxillary, nasal, and zygomatic regions and creates volumetric increases in NPh and MPh airways without altering IPh volume.

Author Contributions

Conceptualization: G.Y. and E.Ö.Ö.; methodology: G.Y. and E.Ö.Ö.; investigation: G.Y.; data curation: G.Y. and E.Ö.Ö.; formal analysis: G.Y. and E.Ö.Ö.; supervision: F.Ö.; writing – original draft: G.Y.; writing – review and editing: E.Ö.Ö. and F.Ö. All authors approved the final version of the manuscript and agree to be accountable for all aspects of the work.

Funding

The authors have nothing to report.

Ethics Statement

This retrospective study was approved by the Marmara University Faculty of Medicine Clinical Research Ethics Committee (Protocol no: 09.2023.1237, 06.10.2023) and conducted in accordance with the Declaration of Helsinki.

Consent

Informed consent was obtained from the parents or legal guardians of all individuals included in the study.

Conflicts of Interest

The authors declare no conflicts of interest.

Data Availability Statement

De-identified data are available from the corresponding author upon reasonable request.

References

1. J. Meyns, J. Meewis, F. Dons, et al., "Long-Term Comparison of Maxillary Protraction With Hybrid Hyrax-Facemask vs. Hybrid Hyrax-Mentoplate Protocols Using Alt-RAMEC: A 5-Year Randomized Controlled Trial," *European Journal of Orthodontics* 47, no. 2 (2025): cjaf011.

2. T. Baccetti, L. Franchi, and J. A. McNamara, Jr., "Treatment and Post-treatment Craniofacial Changes After Rapid Maxillary Expansion and Facemask Therapy," *American Journal of Orthodontics and Dentofacial Orthopedics* 118, no. 4 (2000): 404–413.

3. N. E. Tarraf, O. Dalci, K. Dalci, A. T. Altug, and M. A. Darendeliler, "A Retrospective Comparison of Two Protocols for Correction of Skeletal Class III Malocclusion in Prepubertal Children: Hybrid Hyrax Expander With Mandibular Miniplates and Rapid Maxillary Expansion With Face Mask," *Progress in Orthodontics* 24, no. 1 (2023): 3.

4. P. Ngan, "Early Timely Treatment of Class III Malocclusion," *Seminars in Orthodontics* 11, no. 3 (2005): 140–145.

5. A. J. Kapust, P. M. Sinclair, and P. K. Turley, "Cephalometric Effects of Face Mask/Expansion Therapy in Class III Children: A Comparison of Three Age Groups," *American Journal of Orthodontics and Dentofacial Orthopedics* 113, no. 2 (1998): 204–212.

6. P. Ngan, B. Wilmes, D. Drescher, C. Martin, B. Weaver, and E. Gunel, "Comparison of Two Maxillary Protraction Protocols: Tooth-Borne Versus Bone-Anchored Protraction Facemask Treatment," *Progress in Orthodontics* 16 (2015): 26.

7. Ç. Şar, A. Arman-Özçırpıcı, S. Uçkan, and A. C. Yazıcı, "Comparative Evaluation of Maxillary Protraction With or Without Skeletal Anchorage," *American Journal of Orthodontics and Dentofacial Orthopedics* 139, no. 5 (2011): 636–649.

8. D. Kaya, I. Kocadereli, B. Kan, and F. Tasar, "Effects of Facemask Treatment Anchored With Miniplates After Alternate Rapid Maxillary

Expansions and Constrictions; a Pilot Study," *Angle Orthodontist* 81, no. 4 (2011): 639–646.

9. J. H. Willmann, M. Nienkemper, N. E. Tarraf, B. Wilmes, and D. Drescher, "Early Class III Treatment With Hybrid-Hyrax-Facemask in Comparison to Hybrid-Hyrax-Mentoplate–Skeletal and Dental Outcomes," *Progress in Orthodontics* 19, no. 1 (2018): 42.

10. H. De Clerck, L. Cevidanes, and T. Baccetti, "Dentofacial Effects of Bone-Anchored Maxillary Protraction: A Controlled Study of Consecutively Treated Class III Patients," *American Journal of Orthodontics and Dentofacial Orthopedics* 138, no. 5 (2010): 577–581.

11. Ç. Şar, Z. Şahinoğlu, A. A. Özçırpıcı, and S. Uçkan, "Dentofacial Effects of Skeletal Anchored Treatment Modalities for the Correction of Maxillary Retrognathia," *American Journal of Orthodontics and Dentofacial Orthopedics* 145, no. 1 (2014): 41–54.

12. F. Miranda, D. Garib, F. Pugliese, J. C. da Cunha Bastos, G. Janson, and J. M. Palomo, "Upper Airway Changes in Class III Patients Using Miniscrew-Anchored Maxillary Protraction With Hybrid and Hyrax Expanders: A Randomized Controlled Trial," *Clinical Oral Investigations* 26, no. 1 (2022): 183–195.

13. T. Nguyen, H. De Clerck, M. Wilson, and B. Golden, "Effect of Class III Bone Anchor Treatment on Airway," *Angle Orthodontist* 85, no. 4 (2015): 591–596.

14. R. Steegman, A. Schoeman, A. Dieters, et al., "Three-Dimensional Volumetric Changes in the Airway of Growing Unilateral Complete Cleft Lip and Palate Patients After Bone-Anchored Maxillary Protraction," *American Journal of Orthodontics and Dentofacial Orthopedics* 162, no. 6 (2022): 850–860.

15. S. M. Adel, B. A. Abbas, W. W. Marzouk, and A. R. Zaher, "Airway Dimensional Changes Following Bone Anchored Maxillary Protraction: A Systematic Review," *BMC Oral Health* 23, no. 1 (2023): 260.

16. V. Katyal, B. Wilmes, M. Nienkemper, M. A. Darendeliler, W. Sampson, and D. Drescher, "The Efficacy of Hybrid Hyrax-Mentoplate Combination in Early Class III Treatment: A Novel Approach and Pilot Study," *Australian Orthodontic Journal* 32, no. 1 (2016): 88–96.

17. G. Yıldırım, E. O. Ozbilen, and F. Özdemir, "Retrospective 3-Dimensional Evaluation of Skeletal and Dental Structures Following Treatment With Hybrid Hyrax-Mentonplate With Class III Elastics in Class III Patients With Vertical Growth Pattern: A Pilot Study," *European Journal of Research in Dentistry* 7, no. 2 (2023): 79–88.

18. G. Yıldırım and E. Ö. Özbilen, "Assessment of Maxillary Molar Tooth Changes Caused by Class III Elastics in Hybrid Hyrax-Mentoplate Treatments: A Pilot Study," *Turkish Journal of Orthodontics* 38, no. 1 (2025): 1–11.

19. B. Wilmes, M. Nienkemper, B. Ludwig, C. H. Kau, and D. Drescher, "Early Class III Treatment With a Hybrid Hyrax-Mentoplate Combination," *Journal of Clinical Orthodontics* 45, no. 1 (2011): 15–21.

20. A. Fedorov, R. Beichel, J. Kalpathy-Cramer, et al., "3D Slicer as an Image Computing Platform for the Quantitative Imaging Network," *Magnetic Resonance Imaging* 30, no. 9 (2012): 1323–1341.

21. A. C. de Oliveira Ruellas, C. Tonello, L. R. Gomes, et al., "Common 3-Dimensional Coordinate System for Assessment of Directional Changes," *American Journal of Orthodontics and Dentofacial Orthopedics* 149, no. 5 (2016): 645–656.

22. F. Miranda, S. Barone, M. Gillot, et al., "Artificial Intelligence Applications in Orthodontics," *Journal of the California Dental Association* 51, no. 1 (2023): 2195585.

23. M. Gillot, B. Baquero, C. Le, et al., "Automatic Multi-Anatomical Skull Structure Segmentation of Cone-Beam Computed Tomography Scans Using 3D UNETR," *PLoS One* 17, no. 10 (2022): e0275033.

24. P. W. Ngan, U. Hagg, C. Yiu, and S. H. Wei, "Treatment Response and Long-Term Dentofacial Adaptations to Maxillary Expansion and Protraction," *Seminars in Orthodontics* 3, no. 4 (1997): 255–264.

25. C. Pavoni, C. Masucci, S. Cerroni, L. Franchi, and P. Cozza, "Short-Term Effects Produced by Rapid Maxillary Expansion and Facemask Therapy in Class III Patients With Different Vertical Skeletal Relationships," *Angle Orthodontist* 85, no. 6 (2015): 927–933.

26. P. Cozza, T. Baccetti, M. Mucedero, C. Pavoni, and L. Franchi, "Treatment and Posttreatment Effects of a Facial Mask Combined With a Bite-Block Appliance in Class III Malocclusion," *American Journal of Orthodontics and Dentofacial Orthopedics* 138, no. 3 (2010): 300–310.

27. M. Nienkemper, B. Wilmes, A. Pauls, and D. Drescher, "Maxillary Protraction Using a Hybrid Hyrax-Facemask Combination," *Progress in Orthodontics* 14, no. 1 (2013): 5.

28. M. Nienkemper, B. Wilmes, L. Franchi, and D. Drescher, "Effectiveness of Maxillary Protraction Using a Hybrid Hyrax-Facemask Combination: A Controlled Clinical Study," *Angle Orthodontist* 85, no. 5 (2015): 764–770.

29. S. Liang, F. Wang, Q. Chang, and Y. Bai, "Three-Dimensional Comparative Evaluation of Customized Bone-Anchored vs Tooth-Borne Maxillary Protraction in Patients With Skeletal Class III Malocclusion," *American Journal of Orthodontics and Dentofacial Orthopedics* 160, no. 3 (2021): 374–384.

30. M. H. Elnagar, E. Elshourbagy, S. Ghobashy, M. Khedr, and C. A. Evans, "Comparative Evaluation of 2 Skeletally Anchored Maxillary Protraction Protocols," *American Journal of Orthodontics and Dentofacial Orthopedics* 150, no. 5 (2016): 751–762.

31. J. A. Facio-Umaña, J. Chaurand, and P. I. Gonzalez-Luna, "Early Class III Treatment With Maxillary Protraction-Miniscrew-Assisted Rapid Palatal Expansion (MARPE) and Mandibular Miniplates," *Advances in Oral and Maxillofacial Surgery* 4 (2021): 100151.

32. L. H. Cevidanes, M. A. Styner, and W. R. Proffit, "Image Analysis and Superimposition of 3-Dimensional Cone-Beam Computed Tomography Models," *American Journal of Orthodontics and Dentofacial Orthopedics* 129, no. 5 (2006): 611–618.

33. L. H. Cevidanes, G. Heymann, M. A. Cornelis, H. J. DeClerck, and J. C. Tulloch, "Superimposition of 3-Dimensional Cone-Beam Computed Tomography Models of Growing Patients," *American Journal of Orthodontics and Dentofacial Orthopedics* 136, no. 1 (2009): 94–99.

34. N. Mandall, R. Cousley, A. DiBiase, et al., "Early Class III Protraction Facemask Treatment Reduces the Need for Orthognathic Surgery: A Multi-Centre, Two-Arm Parallel Randomized, Controlled Trial," *Journal of Orthodontics* 43, no. 3 (2016): 164–175.

35. F. Miranda, J. C. da Cunha Bastos, A. M. Dos Santos, G. Janson, J. R. P. Lauris, and D. Garib, "Dentoskeletal Comparison of Miniscrew-Anchored Maxillary Protraction With Hybrid and Conventional Hyrax Expanders: A Randomized Clinical Trial," *American Journal of Orthodontics and Dentofacial Orthopedics* 160, no. 6 (2021): 774–783.

36. C. Bastiani, S. A. Bellini-Pereira, A. Aliaga-Del Castillo, K. Chiqueto, J. F. Castanha Henriques, and G. Janson, "Authors' Response," *American Journal of Orthodontics and Dentofacial Orthopedics* 164, no. 3 (2023): 305–306.

37. F. Miranda, D. Garib, I. Silva, et al., "Maxillary Protraction Anchored on Miniplates Versus Miniscrews: Three-Dimensional Dentoskeletal Comparison," *European Journal of Orthodontics* 47, no. 1 (2025): cjae071.

38. T. Ergul and A. Gulec, "Comparison of the Effectiveness of Skeletal and Tooth-Borne Protraction Methods With or Without Alternate Rapid Maxillary Expansion and Constriction Protocol in Patients With Class III Malocclusion," *American Journal of Orthodontics and Dentofacial Orthopedics* 167, no. 3 (2025): 282–295.

39. V. Pangrazio-Kulbersh, P. Wine, M. Haughey, B. Pajtas, and R. Kaczynski, "Cone Beam Computed Tomography Evaluation of Changes in the Naso-Maxillary Complex Associated With Two Types of Maxillary Expanders," *Angle Orthodontist* 82, no. 3 (2012): 448–457.